BJR

https://doi.org/10.1259/bjr.20190373

Received: 22 April 2019 | Revised: 18 June 2019 | Accepted: 21 July 2019

Cite this article as:
Sun Y, Williams S, Byrne D, Keam S, Reynolds HM, Mitchell C, et al. Association analysis between quantitative MRI features and hypoxia-related genetic profiles in prostate cancer: a pilot study. *Br J Radiol* 2019; **92**: 20190373.

SHORT COMMUNICATION

Association analysis between quantitative MRI features and hypoxia-related genetic profiles in prostate cancer: a pilot study

[1,2]YU SUN, [2,3]SCOTT WILLIAMS, [3]DAVID BYRNE, [3]SIMON KEAM, [2,3]HAYLEY M. REYNOLDS, [3]CATHERINE MITCHELL, [4]DARREN WRAITH, [2,3]DECLAN MURPHY and [1,2]ANNETTE HAWORTH

[1]The University of Sydney, Sydney, New South Wales, Australia
[2]The Sir Peter MacCallum Department of Oncology, The University of Melbourne, Melbourne, Victoria, Australia
[3]Peter MacCallum Cancer Centre, Melbourne, Victoria, Australia
[4]Queensland University of Technology, Brisbane, Queensland, Australia

Address correspondence to: Yu Sun
E-mail: *yu.sun@sydney.edu.au*

Objective: To investigate the association between multiparametric MRI (mpMRI) imaging features and hypoxia-related genetic profiles in prostate cancer.
Methods: *In vivo* mpMRI was acquired from six patients prior to radical prostatectomy. Sequences included T_2 weighted (T_2W) imaging, diffusion-weighted imaging, dynamic contrast enhanced MRI and blood oxygen-level dependent imaging. Imaging data were co-registered with histology using three-dimensional deformable registration methods. Texture features were extracted from T_2W images and parametric maps from functional MRI. Full transcriptome genetic profiles were obtained using next generation sequencing from the prostate specimens. Pearson correlation coefficients were calculated between mpMRI data and hypoxia-related gene expression levels. Results were validated using glucose transporter one immunohistochemistry (IHC).
Results: Correlation analysis identified 34 candidate imaging features (six from the mpMRI data and 28 from T_2W texture features). The IHC validation showed that 16 out of the 28 T_2W texture features achieved weak but significant correlations ($p < 0.05$).
Conclusions: Weak associations between mpMRI features and hypoxia gene expressions were found. This indicates the potential use of MRI in assessing hypoxia status in prostate cancer. Further validation is required due to the low correlation levels.
Advances in knowledge: This is a pilot study using radiogenomics approaches to address hypoxia within the prostate, which provides an opportunity for hypoxia-guided selective treatment techniques.

INTRODUCTION

Prostate cancer (PCa) is the most common non-dermatologic malignancy in males.[1] Both surgery and radiation therapy (RT) have demonstrated high rates of biochemical control; however, around 25% of patients eventually develop either local or distal progressive disease.[2] Hypoxia has been widely linked to local and distal failure in several solid tumours treated with RT, and strategies for targeting hypoxia during radiotherapy in several cancers has been shown to improve local control.[3,4] Hypoxia is known to exist in PCa, but assessment is difficult with *in vivo* hypoxia imaging only reported in a limited number of studies.[5–7] Of these, multiparametric MRI (mpMRI), which is widely used for the detection and characterization of PCa,[8] shows the most promise in identifying regions and levels of hypoxia.[5–7]

To develop hypoxia imaging biomarkers, one key barrier is the establishment of "ground truth" data. In the case of prostate cancer, the oxygen electrode (Eppendorf electrode) provides a direct measure of oxygenation, but this method has several limitations. In addition to being invasive, the electrode cannot capture the intratumour heterogeneity. Furthermore, it can only be operated on live or fresh tissues which greatly restricts its use on pathological specimens, typically available in the form of formalin-fixed paraffin embedded (FFPE) samples. To work around such limitations, genetic profiles of the sample may be suitable as a surrogate for hypoxia. The rationale is that hypoxia triggers a defined cascade of molecular responses that can be assessed at the RNA and the protein level. Such changes can then be measured using sequencing methods for RNAs or antibody-based protocols (*e.g.* immunohistochemistry, IHC) for proteins. Using the genetic profiles as surrogates

Figure 1. Study workflow. Step 1: *in vivo* mpMRI data were acquired from six patients prior to radical prostatectomy (Step 2). Step 3: gene sequencing data of predefined ROIs were acquired. Step 4: exploratory analysis using Pearson's correlation coefficient was performed between the corresponding ROI in mpMRI quantitative imaging features (blue panel) and genetic profiles (orange panel) to identify high-performance candidate imaging features. Step 5: IHC staining using GLUT-1 was performed and used to validate the candidate imaging features (Step 6). The corresponding ROIs are shown as circles in the prostate specimen, mpMRI data and texture features. IHC, immunohistochemistry; mpMRI, multiparametricMRI; ROI, region of interest.

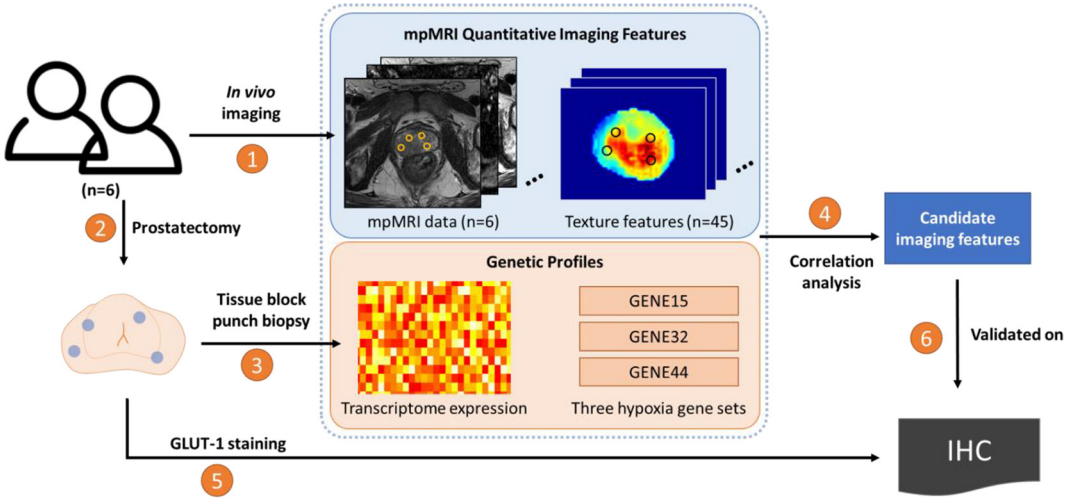

for hypoxia, corresponding features within the imaging data can be correlated to develop predictive imaging biomarkers. This research paradigm, *i.e.* the integrative analysis of both genetic and imaging data, is termed "radiogenomics". In a cervical cancer study by Fjeldbo et al, classification of cancer tissue into either "less hypoxic" or "more hypoxic" was successfully achieved using dynamic contrast-enhanced (DCE)-MRI and a six-gene signature.[9] This suggests that DCE-MRI can be used as an imaging biomarker for cervical cancer hypoxia. Clinical significance of this study was demonstrated as the "more hypoxic" patient cohort had poorer progression-free survival probability compared to the "less hypoxic" group.[9] However, the feasibility of such methods remains unknown for PCa.

The aim of this study was to investigate the correlation between mpMRI data and hypoxia-related gene expressions in PCa. We hypothesise that imaging data from mpMRI, including T_2 weighted (T_2W) imaging, diffusion-weighted imaging (DWI) and DCE-MRI, contain sufficient information to correlate with tissue hypoxia status characterised by genetic profiles and confirmed using an immunohistochemical marker of hypoxia. Our intention was to identify potential imaging biomarkers for defining hypoxic regions in PCa for use in biological optimisation approaches in prostate radiotherapy.[10]

METHODS AND MATERIALS

This study was approved by our institutional Human Research Ethics Committee (HREC/15/PMCC/125) and informed consent was obtained from all patients. The workflow is shown in Figure 1. Six patients (demographics in Table 1) scheduled for radical prostatectomy (RP) were recruited prospectively at the Peter MacCallum Cancer Centre (PMCC) in Melbourne, Australia.

MRI acquisition and processing

In vivo MRI acquisition

In vivo mpMRI scans (details in Supplementary Material 1, S1) were acquired prior to radical prostatectomy using a 3 T Siemens Trio Tim scanner (Siemens Medical Solutions,

Table 1. Patient demographics

Patient	Age	PSA (ng·ml^{-1})	Gleason score (dominant nodule)	Pathological stage	Tumour volume (mm^3)	Number of sequencing samples
1	69	6.3	3 + 4=7	pT2c	2500	6
2	63	11.0	4 + 3=7	pT3a	2000	8
3	71	4.3	3 + 4=7	pT3a N0	2000	6
4	62	6.1	3 + 4=7	pT3a N0	3900	6
5	65	6.2	3 + 4=7	pT2c	1900	6
6	66	5.0	3 + 4=7	pT2c Nx	4500	6

PSA, prostate specific antigen.

Erlangen, Germany). Sequences included T_2W imaging, DWI and DCE-MRI according to the European Society of Urogenital Radiology guidelines.[11] Apparent diffusion coefficient (ADC) maps were computed from DWI data and four pharmacokinetic maps including volume transfer constant (K^{trans}), interstitium-to-plasma rate constant (k_{ep}), extracellular extravascular volume fraction (V_e) and initial area under the curve (IAUC) were computed by fitting the Tofts model to the DCE data. We also acquired BOLD-MRI data based on the report by Hoskin et al who described its potential use in assessing hypoxia.[5] R2* maps were computed from BOLD-MRI and incorporated in the analysis. *In vivo* three-dimensional T_2W images were acquired to aid the registration with histology.

Feature extraction

Texture features (TFs) were computed from *in vivo* two-dimensional T_2W images (R Statistical Software v. 3.1). These included four statistical families: gray-level co-occurrence matrix (GLCM, $n = 21$), gray-level run length matrix (GLRLM, $n = 11$), gray-level size zone matrix (GLSZM, $n = 11$) and local binary patterns (LBP, $n = 2$). A full list of TFs is shown in Supplementary Material 1, S2. Prior to feature extraction, N4 normalisation was applied on T_2W images for bias-field correction, followed by standardization using Z-scores to reduce patient variability.

Histology

After radical prostatectomy, the prostate specimen was weighed, inked and formalin-fixed. Three microtomed sections of 3 µm thickness (L1, L2 and L3) were obtained from the prostate tissue block, as is shown in Figure 2. The L1 histology section was Haematoxylin and Eosin (H&E) stained, and an experienced uropathologist (CM) annotated the tumour and reported with Gleason Scores according to standard clinical practice.

Registration

Parametric maps computed from the *in vivo* mpMRI data (ADC, K^{trans}, k_{ep}, V_e, IAUC and R2*) were rigidly registered with *in vivo* two-dimensional T_2W images. L1 histology was co-registered with *in vivo* mpMRI data using the registration framework of Reynolds et al..[12] This method utilises *ex vivo* T_2W images of the prostate specimen and deformable image registration of three-dimensional *in vivo* and *ex vivo* T_2W images to account for non-uniform shrinkage and post-surgical deformations. L2 and L3 histology were then rigidly co-registered with L1 histology (indicated by arrows in Figure 2).

Genetic profiling

Next generation sequencing

Punch biopsies were performed on the prostate tissue blocks (Supplementary Material 1, S3). A total of 38 punch cores were collected. For each punch core, RNA was isolated and purified

Figure 2. Schematic diagram showing the prostate tissue block and histology sections (L1, L2 and L3). The L1 histology section was used to annotate the tumour and select suitable positions for punch biopsies. The L2 histology section was reserved for the IHC staining in the validation study, and L3 (obtained after the punch biopsy) was used to determine the actual position of the punch biopsies. Image registration (shown by arrows) was carried out between L2 and L1, L3 and L1, and then all histology sections were co-registered with mpMRI data via L1. IHC, immunohistochemistry; mpMRI, multiparametric MRI.

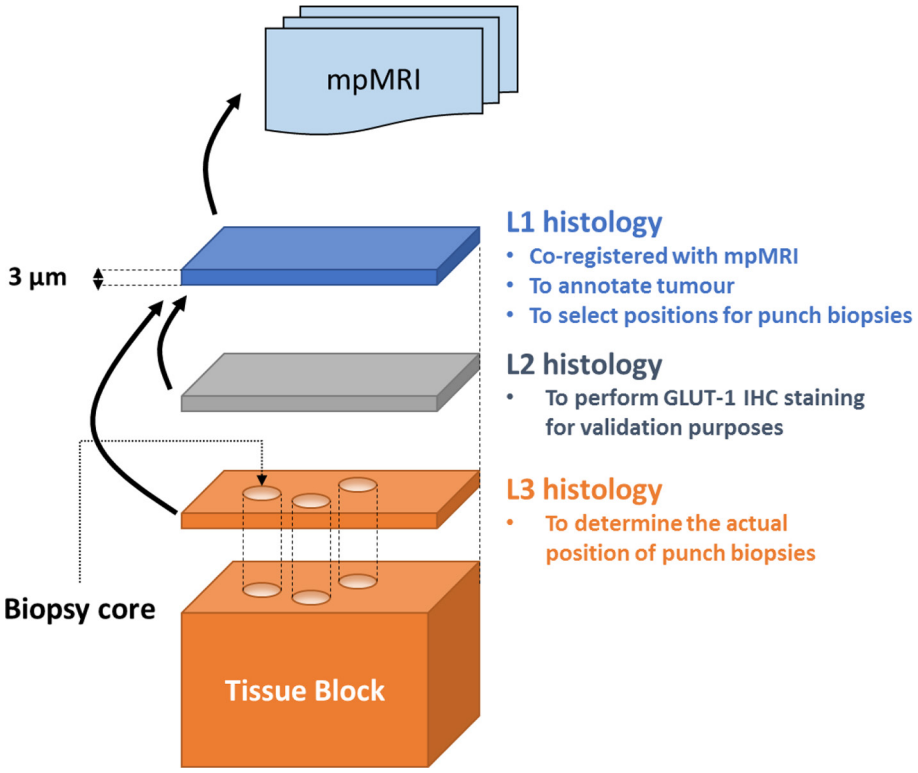

from core punches using the RNeasy FFPE kit (Qiagen, Hilden, Germany) according to the manufacturer's instructions. Quality assurance was performed by testing 1 µl of RNA from validation samples using a High Sensitivity RNA TapeStation assay (Agilent, Santa Clara). Genome-wide transcriptomic analyses were performed using 5 µl of DNAse-treated input RNA for library generation using a QuantSeq 3' mRNA-Seq library kit (Lexogen, Vienna, Austria). NGS sequencing was performed on a NextSeq HO 75SE run at the Molecular Genomics Facility at the PMCC. Sequenced samples were aligned using TopHat v 2.1.1 and quantified using Htseq v. 0.6.1 software. Normalization was performed with Limma-Voom in R v. 3.3.3 using punch biopsy samples from regions of tumours, benign tissues and the margins..

Hypoxia-related gene sets

Three hypoxia-related gene sets were selected for investigation based on previous studies. These included: (1) a 15-gene universal hypoxia gene set, (GENE15),[13] (2) a 32-gene prostate specific hypoxia gene set defined by Ragnum et al. (GENE32)[14] and (3) a 44-gene high frequency hypoxia gene set summarized from previous literatures (details in Supplementary Material 1, S4). GENE44 included HIF1A and VEGFA which were not present in either GENE15 or GENE32.

Correlation analysis

Sample preparation

To determine the punch biopsy positions relative to the L1 histology, the L3 histology section was microtomed after the punch biopsies were carried out (Figure 2). The L3 histology slides were co-registered with L1 histology using rigid registration. Biopsy positions located on L3 were defined as regions of interest (ROIs) and subsequently propogated to the co-registered mpMRI data. A dilation of 2 mm was performed to reduce the impact from registration uncertainty. Each ROI was considered as one sample in the analysis, which had corresponding mpMRI data and genomic data.

Table 2. High-performance genes and the number of significant correlations with mpMRI quantitative imaging features

Gene Set	Gene	Frequency
GENE15	PFKFB3	11
	P4HA2	6
GENE32	DDIT4	7
	TNFSF13B	7
GENE44	AKAP12	13
	NFIL3	13
	SERPINE1	13
	VEGFA	13
	KLF6	12
	MAFF	12
	EDN1	11
	HIF1A	10
	IGFBP3	7
	TXNIP	7
	ATF3	6
	PFKP	5

Statistical analysis

Pearson correlation coefficients (ρ) were computed between mpMRI imaging features and hypoxia-related genes (R Statistical Software v. 3.2, Vienna, Austria). A pool of candidate imaging features was empirically defined using a rho threshold (ρ >0.30).

Validation

Acknowledging that genetic profiles are surrogates for hypoxia, a subsequent analysis was performed to validate the results in the correlation analysis. IHC staining was performed using the hypoxia marker glucose transporter 1 (GLUT-1). L2 histology was used for IHC staining. Pearson correlation coefficients between candidate feature images and GLUT-1 IHC were computed at

Figure 3. Heatmap showing the correlation between mpMRI quantitative imaging features and expression levels of genes from GENE15. (Acronyms defined according to Supplementary Material 1, S2).

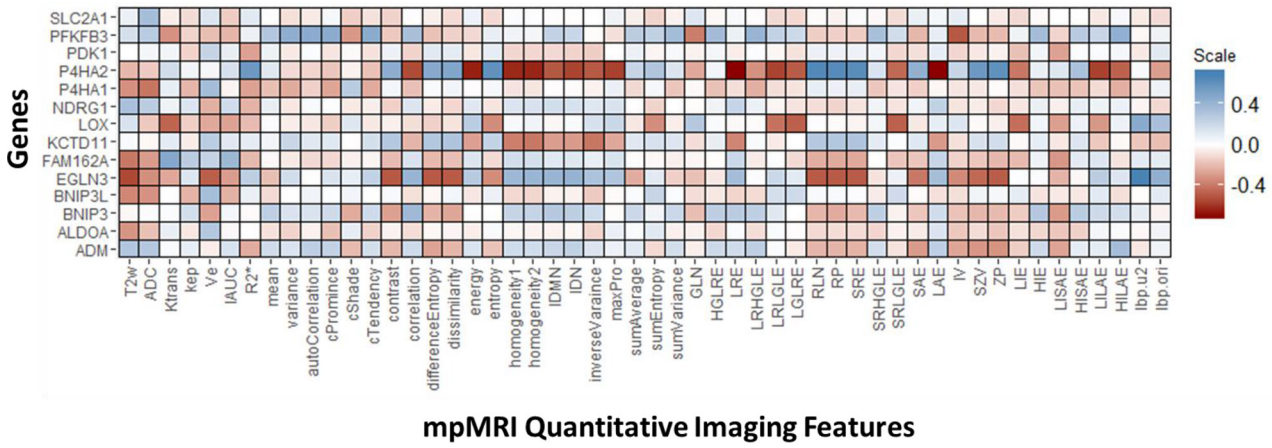

Figure 4. Candidate imaging features identified by the correlation analysis, ranked by the number of significant correlation achieved with expression levels of hypoxia-related genes. (Acronyms defined according to Supplementary Material 1, S2)

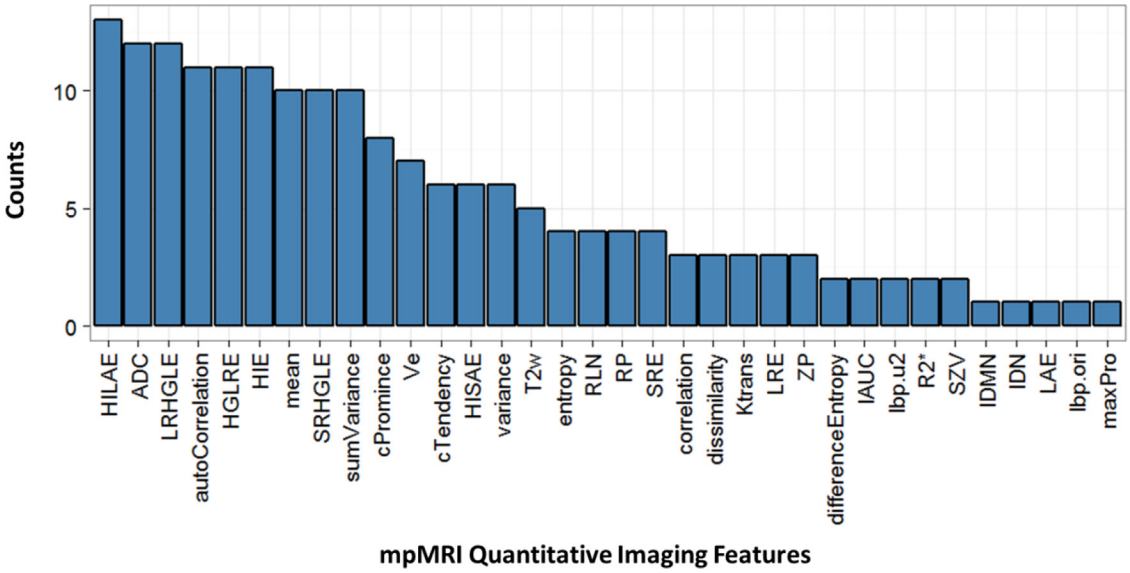

a voxel level using R Statistical Software (v. 3.2). Features were considered valid only if a significant correlation with GLUT-1 was found ($p < 0.05$). Imaging features that correlated with both the gene features and GLUT-1 were classed as "validated" features and potential candidates worthy of further investigation.

RESULTS

Correlation analysis

Pearson correlation coefficients between mpMRI data and hypoxia-related genes are shown as a heat map for GENE15 (Figure 3), GENE32 (Supplementary Material 1, S5) and GENE44 (Supplementary Material 1, S6). Genes which showed a significant moderate-to-high correlation with mpMRI features are given in Table 2. A total of 34 candidate features were identified which included 28 TFs and six mpMRI parametric maps (Figure 4).

Validation

Each of the 34 candidate features was assessed for their correlation significance with GLUT-1 IHC. None of the six mpMRI parametric maps reached significance, while 16 of the 28 TFs from T_2W MRI were confirmed as potential candidates (Figure 5).

DISCUSSION

Hypoxia presents a great challenge in radiation therapy due to increased radioresistance of hypoxic tumour cells. Defining the spatial distribution of hypoxia within a solid tumour provides an opportunity to preferentially target hypoxic regions with high doses of radiation. In the radiation planning study of Haworth et al, it was shown that by using knowledge of the spatial distribution of the tumour phenotype, a biological dose-optimization strategy based on factors including hypoxia distribution

Figure 5. Results of the validation study using GLUT-1 IHC. The dashed line separates the mpMRI images and T_2W texture features. None of the mpMRI images achieved significant correlation, while 16 of 28 texture features achieved significant correlation. (Acronyms defined according to Supplementary Material 1, S2)

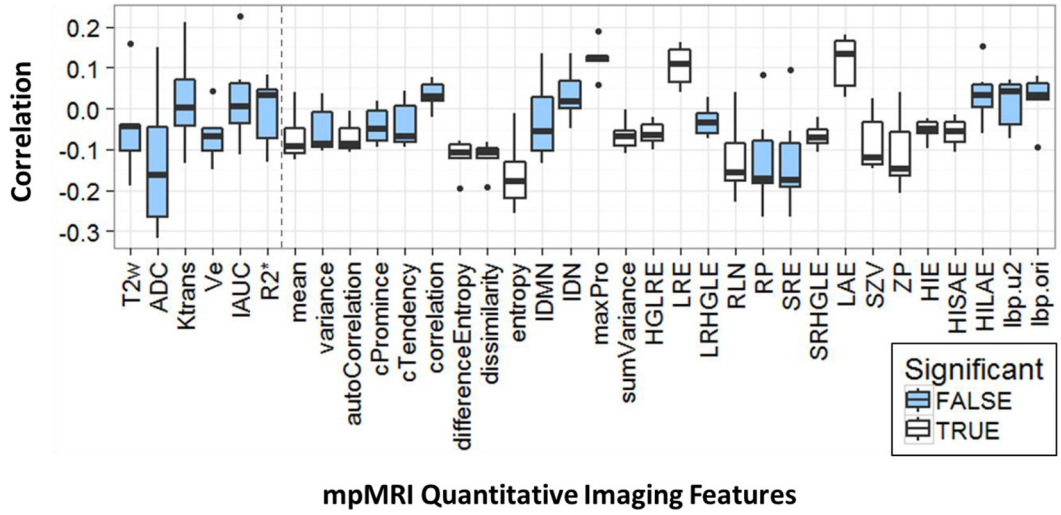

can optimize tumour control probability whilst sparing normal tissue.[10] The model requires voxel-wise descriptors of tumour biology and was the motivation for the current study.[10] We used a radiogenomics approach with hypoxia-related gene signatures as surrogates of ground truth similar to the approach used in a study of cancer of the cervix.[9] Our results identified several texture features which were significantly associated with hypoxia-related gene expressions. In the correlation analysis, six features were from the mpMRI images/maps (ADC, Ve, T_2W, Ktrans, IAUC and R2*), while the remaining 28 features were from T_2W image TFs. While none of the mpMRI images / maps passed the validation using IHC, 16 of the TFs from T_2W images showed a significant correlation.

Our study identified several hypoxia-related genes that were strongly associated with mpMRI quantitative imaging features. These included HIF1A, VEGFA, PFKFB3, P4HA2, DDIT3 and ANG (Supplementary Material 1, S4). Similarly in the cervical cancer study of Fjeldbo et al,[9] P4HA2 and DDIT4 were also found to correlate with imaging features. These genes are strongly related to cellular structure and tissue development which forms a plausible link between genomic data and T_2W texture features, as T_2W images are mainly dependent on tissue structures. These structure-related genes included: (1) P4HA2, the gene encoding part of the collagen synthesis enzyme, with collagen being an important material for cellular structures; (2) DDIT4, a negative regulator of mTOR which can regulate growth, proliferation and autophagy; (3) SERPINE1, a serine protease inhibitor protein for urokinase, which activates fibrinolysis (blood clot breakdown); (4) VEGFA, an important growth factor for epithelial cells and a main inducer for blood vessel growth; (5) END1, a potent modulator for blood vessel narrowing (vasoconstriction) and (6) ANG, a stimulator for blood vessel development through the process of angiogenesis.

This is a first-in-human pilot study to integrate radiogenomics in the selection of features relevant to hypoxia. Hompland et al used the exogenous hypoxia marker pimonidazole as the surrogate and found a correlation with a novel consumption and supply map from DWI.[6] However, their imaging protocol was beyond the standard European Society of Urogenital Radiology guidelines and hence not investigated in the current study. Similarly, Hoskin et al found a correlation between R2* from BOLD imaging and pimonidazole markers. In our results, R2* was not found to significantly correlated with the genetic profiles.[5]

Whilst hypoxic cells can be two to three times more radioresistant than normoxic cells, there is no consensus on the general benefit of dose intensification for prostate hypoxia.[15] Milosevic et al,[2] in a study of 247 patients, demonstrated a relationship between pre-treatment hypoxia and local recurrence following radiotherapy, however this study was not powered to determine the influence of radiation dose. As noted by Bristow et al,[15] more work is needed to identify patients that would benefit from radiation dose escalation, noting that personalized treatments of the future may also consider the role of systemic agents and androgen-deprivation therapy. We propose that an important part of this strategy will involve monitoring tumour heterogeneity before, during and following radiotherapy, and non-invasive methods such as those described in this study, will play an important role in defining these subgroups of patients. Furthermore, we believe brachytherapy, in particular, high-dose-rate brachytherapy, will be an ideal treatment modality to achieve accurate delivery of highly conformal dose distributions due to the high dose gradients surrounding a radioactive source.

There are several limitations in this exploratory study. First, there was an average registration uncertainty of 3.3 mm between mpMRI data and histology. To account for this, a margin was applied to the imaging ROIs using the methods of Reynolds et al. However, the impact of registration uncertainty was intrinsic in the data and could not be fully eliminated. Whilst multiple correlation testing was not applied in the analysis, which may increase the chance of false discoveries—an issue common to all studies of this nature, this study aimed to identify potential biomarkers for further investigation. Hence, false discovery was less relevant in this setting and multiple correlation testing will be applied in future validation studies using a different patient cohort. Lastly, due to the small patient cohort size, the resulting data were insufficient for building a predictive model. Therefore, this study serves as a "feature selection" step, identifying the significant value of texture features in contrast to the mpMRI parametric maps. Future work will start from this pool with a goal to develop predictive models to stratify hypoxia status into binary categories (more hypoxic/less hypoxic). The output from the model can be integrated into clinical procedures by increasing the dose in hypoxic subvolumes to account for radioresistance in hypoxic regions,[2] which may lead to better patient outcome.

CONCLUSION

The association between mpMRI quantitative imaging features and hypoxia status was investigated, using a radiogenomics approach. Exploratory analysis identified 16 promising T_2W texture features which achieved significant correlations with hypoxia-related genetic profiles using both sequencing and IHC techniques. Whilst further validation is required in a larger cohort of patients, this is the first-in-human attempt to apply radiogenomics approaches in PCa patients to spatially evaluate hypoxia.

ACKNOWLEDGMENT

This study is supported by NHMRC (grant 1126955), PdCCRS (grant 628592) with funding partners: Prostate Cancer Foundation of Australia, and the Radiation Oncology Section of the Australian Government of Health and Aging and Cancer Australia. Yu Sun is funded by the Melbourne International Research Scholarship, a Movember Young Investigator Grant through Prostate Cancer Foundation of Australia (PCFA) and Cancer Therapeutics Top-up Funding. Hayley Reynolds is funded by a Movember Young Investigator Grant through PCFA's Research Program. The authors would like to thank Courtney Savill for prostate specimen processing and Lauren Caspersz for mpMRI acquisitions.

REFERENCES

1. Siegel RL, Miller KD, Jemal A, statistics C. Cancer statistics, 2016. *CA Cancer J Clin* 2016; **66**: 7–302016. doi: https://doi.org/10.3322/caac.21332
2. Milosevic M, Warde P, Ménard C, Chung P, Toi A, Ishkanian A, et al. Tumor hypoxia predicts biochemical failure following radiotherapy for clinically localized prostate cancer. *Clin Cancer Res* 2012; **18**: 2108–14. doi: https://doi.org/10.1158/1078-0432.CCR-11-2711
3. Hoskin PJ, Rojas AM, Bentzen SM, Saunders MI. Radiotherapy with concurrent carbogen and nicotinamide in bladder carcinoma. *JCO* 2010; **28**: 4912–8. doi: https://doi.org/10.1200/JCO.2010.28.4950
4. Overgaard J. Hypoxic modification of radiotherapy in squamous cell carcinoma of the head and neck--a systematic review and meta-analysis. *Radiother Oncol* 2011; **100**: 22–32. doi: https://doi.org/10.1016/j.radonc.2011.03.004
5. Hoskin PJ, Carnell DM, Taylor NJ, Smith RE, Stirling JJ, Daley FM, et al. Hypoxia in prostate cancer: correlation of BOLD-MRI with pimonidazole immunohistochemistry-initial observations. *Int J Radiat Oncol Biol Phys* 2007; **68**: 1065–71. doi: https://doi.org/10.1016/j.ijrobp.2007.01.018
6. Hompland T, Hole KH, Ragnum HB, Aarnes E-K, Vlatkovic L, Lie AK, et al. Combined MR imaging of oxygen consumption and supply reveals tumor hypoxia and aggressiveness in prostate cancer patients. *Cancer Res* 2018; **78**: 4774–85. doi: https://doi.org/10.1158/0008-5472.CAN-17-3806
7. Stoyanova R, Ackerstaff E, Cho H, Koutcher JA, Pollack A. Dce-Mri for delineation of hypoxic regions in prostate tumors. *Int J Radiat Oncol Biol Phys* 2010; **78**: S337. doi: https://doi.org/10.1016/j.ijrobp.2010.07.799
8. Johnson LM, Turkbey B, Figg WD, Choyke PL. Multiparametric MRI in prostate cancer management. *Nat Rev Clin Oncol* 2014; **11**: 346–53. doi: https://doi.org/10.1038/nrclinonc.2014.69
9. Fjeldbo CS, Julin CH, Lando M, Forsberg MF, Aarnes E-K, Alsner J, et al. Integrative analysis of DCE-MRI and gene expression profiles in construction of a gene classifier for assessment of hypoxia-related risk of chemoradiotherapy failure in cervical cancer. *Clin Cancer Res* 2016; **22**: 4067–76. doi: https://doi.org/10.1158/1078-0432.CCR-15-2322
10. Haworth A, Williams S, Reynolds H, Waterhouse D, Duchesne GM, Bucci J, et al. Validation of a radiobiological model for low-dose-rate prostate boost focal therapy treatment planning. *Brachytherapy* 2013; **12**: 628–36. doi: https://doi.org/10.1016/j.brachy.2013.04.008
11. Barentsz JO, Richenberg J, Clements R, Choyke P, Verma S, Villeirs G, et al. ESUR prostate Mr guidelines 2012. *Eur Radiol* 2012; **22**: 746–57. doi: https://doi.org/10.1007/s00330-011-2377-y
12. Reynolds HM, Williams S, Zhang A, Chakravorty R, Rawlinson D, Ong CS, et al. Development of a registration framework to validate MRI with histology for prostate focal therapy. *Med Phys* 2015; **42**: 7078–89. doi: https://doi.org/10.1118/1.4935343
13. Sørensen BS, Knudsen A, Wittrup CF, Nielsen S, Aggerholm-Pedersen N, Busk M, et al. The usability of a 15-gene hypoxia classifier as a universal hypoxia profile in various cancer cell types. *Radiother Oncol* 2015; **116**: 346–51. doi: https://doi.org/10.1016/j.radonc.2015.06.028
14. Ragnum HB, Vlatkovic L, Lie AK, Axcrona K, Julin CH, Frikstad KM, et al. The tumour hypoxia marker pimonidazole reflects a transcriptional programme associated with aggressive prostate cancer. *Br J Cancer* 2015; **112**: 382–90. doi: https://doi.org/10.1038/bjc.2014.604
15. Bristow RG, Berlin A, Dal Pra A. An arranged marriage for precision medicine: hypoxia and genomic assays in localized prostate cancer radiotherapy. *Br J Radiol* 2014; **87**: 20130753. doi: https://doi.org/10.1259/bjr.20130753